Chinese Chemical Letters 35 (2024) 108947

Contents lists available at ScienceDirect

Chinese Chemical Letters

journal homepage: www.elsevier.com/locate/cclet

Nucleus-targeting orange-emissive carbon dots delivery adriamycin for enhanced anti-liver cancer therapy

Qiang Li[a,b,1], Jiangbo Fan[b,1], Hongkai Mu[b], Lin Chen[c,d], Yongzhen Yang[c,d,*], Shiping Yu[b,*]

[a] The Second Hospital of Shanxi Medical University, Taiyuan 030001, China
[b] Shanxi Medical University, Taiyuan 030001, China
[c] Key Laboratory of Interface Science and Engineering in Advanced Materials, Ministry of Education, Taiyuan University of Technology, Taiyuan 030024, China
[d] Shanxi-Zheda Institute of Advanced Materials and Chemical Engineering, Taiyuan 030032, China

ARTICLE INFO

Article history:
Received 5 July 2023
Revised 16 August 2023
Accepted 17 August 2023
Available online 19 August 2023

Keywords:
Carbon dots
Nucleus-targeting
Adriamycin
Drug delivery system
Liver cancer therapy

ABSTRACT

Carbon dots (CDs) with precise targeting function show great potential in the field of drug delivery therapeutics. In this study, the functionalized nucleus-targeting orange-emissive CDs with nuclear localization sequence (NLS) were loaded with adriamycin (DOX) to obtain a nucleus-targeting orange-emissive CDs drug delivery system (CDs-NLS-DOX), which delivered DOX to tumor cell nuclei to enhance its anti-tumor activity. The drug carrier orange-emissive CDs showed excitation-independent behavior, stable and enhanced imaging capability and good biocompatibility *in vitro* and *in vivo*. Meanwhile, the CDs-NLS could target the nuclei efficiently, and the CDs-NLS-DOX complexes had a high drug loading rate (59.4%) after loading DOX, exhibiting pH-dependent DOX release behavior through breaking acylhydrazone bond in a weak acidic environment. In addition, the CDs-NLS-DOX complexes exhibited an enhanced killing activity against human hepatoma cells (HepG2). The *in vivo* therapeutic effects on HepG2 nude mice transplanted tumors indicated the CDs-NLS-DOX had a stronger ability to inhibit tumor growth compared to free DOX. In short, CDs-NLS-DOX is expected to be a precise and efficient nucleus-targeting nano-drug delivery system for tumor treatment.

Liver cancer is currently the fourth most common malignant tumor and the second leading cause of death in China, as well as a major global public health problem, seriously threatening people's lives and health safety [1]. The latency of initial onset and the long asymptomatic period led to the fact that some patients have already progressed to the middle and late stages when liver cancer is discovered, and even developed into malignant disease, which is often no longer suitable for surgical resection or liver transplantation [2]. In recent years, chemotherapy has been paid increasing attention in the treatment of liver cancer.

However, liver cancer chemotherapy is currently facing two major challenges. On the one hand, the indiscriminate distribution of chemotherapeutic drugs in non-tumor areas can cause the different degrees of damage to normal cells as well, which interferes with the growth and metabolism of normal tissue cells, resulting in the gastrointestinal toxicity in mild cases and even the bone marrow suppression in severe cases [3]. On the other hand, the prolonged use of chemotherapeutic drugs can activate the expression of drug efflux protein (P-gp) on the surface of tumor cell membranes, which can reverse the intracellular chemotherapeutic drug transport out of tumor cells, resulting in multidrug-resistance [4]. Therefore, it is imperative to accumulate high concentration of drug in the tumor region without increasing systemic drug concentration, and prevent multidrug-resistance by minimizing the expression of P-gp on the surface of tumor cell membranes. In order to meet this requirement for addressing the above two challenges, an ideal drug delivery system should be developed to deliver the drugs. It must have a strong affinity for the target tissue or cells, and the timed release of intracellular drug localization, which will realize selectable and controllable ability of drug delivery, not only improving drug efficacy, but also reducing systemic drug toxicity to improve patients' quality of life.

In recent years, the emergence of organelle targeting nano delivery systems has provided a turnaround for tumor potentiation and toxicity reduction [5,6], which is a combination of nanocarriers, organelle targeting molecules, and therapeutic drugs. They can target tumor-specific organelles and release drugs accurately, which is expected to improve the bioavailability of drugs and

* Corresponding authors.
E-mail addresses: yyztyut@126.com (Y. Yang), yushiping6@126.com (S. Yu).
[1] These authors contributed equally to this work.

https://doi.org/10.1016/j.cclet.2023.108947
1001-8417/

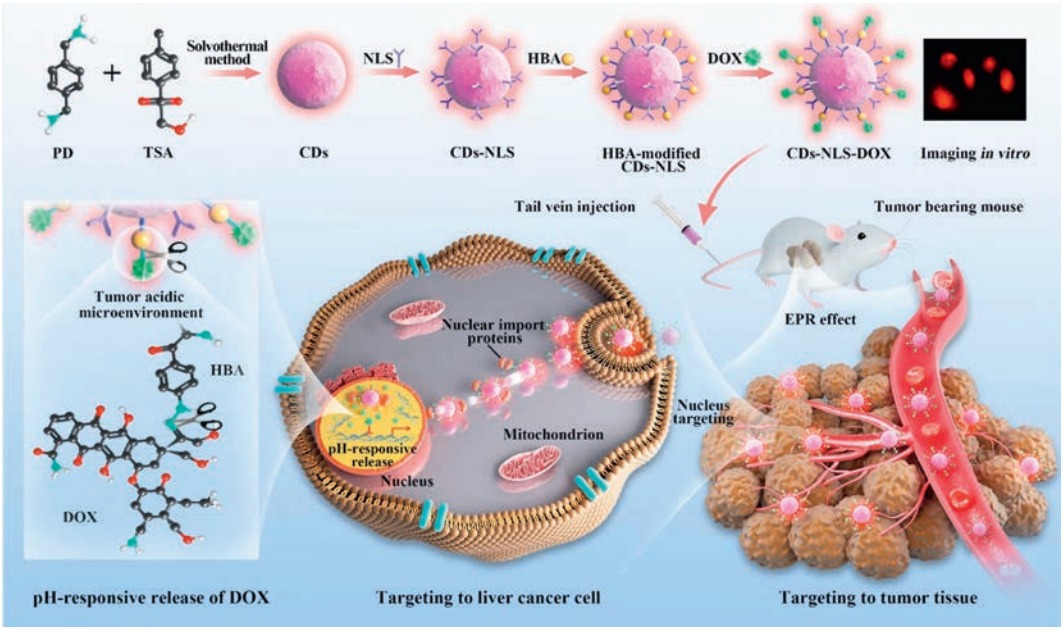

Scheme 1. Schematic of the synthesis CDs-NLS-DOX and their delivery of DOX and imaging for liver cancer target therapy.

achieve precise and effective treatment for tumors. Based on this, the research on nucleus-targeting nanodrug delivery systems is increasing year by year [7–9]. The reason lies in the following two aspects. First, nuclei are the storage center of cellular genetic materials and the site of protein transcription, and the DNA in nuclei is the final action site of many chemotherapeutic drugs [10,11]. Second, chemotherapeutic drugs are transported directly into nuclei, evading the pathway of the P-gp-mediated drug resistance in cell membrane, which is expected to reduce drug efflux and increase intracellular drug concentration [12]. At present, the research on nucleus-targeting drug delivery has made some progress, but still faces some obstacles, in which the selection of high-quality nanocarriers and precise nucleus-targeting molecules are the two major challenges.

At present, the nanocarriers that can be used for nucleus-targeting drug delivery mainly include inorganic nanocarriers, lipid nanocarriers and polymeric nanocarriers [13]. Among them, as a kind of novel inorganic carbon nanoparticles, carbon dots (CDs) can be used as effectively targeted nanodrug carriers because of their excellent optical stability, easy surface modification and good biocompatibility [14–16]. CDs can carry a variety of drugs, among which adriamycin (DOX) is widely used as an anthracycline antibiotic with a wide range of antitumor effect in clinical practice, and its mechanism of action is to interfere with the replication of DNA in nuclei and thus induce the apoptosis in tumor cells [17,18]. CDs-based DOX (CDs-DOX) delivery system can selectively accumulate at the tumor site by virtue of enhanced permeability and retention (EPR) effect in solid tumors, thereby increasing the drug concentration in tumor tissues [19,20]. Kong *et al.* [21] prepared a DOX delivery system using CDs as carriers and explored its therapeutic activity. Results showed that CDs-DOX complexes had higher cellular uptake and better *in vitro* antitumor effect on human breast cancer cells MCF-7 compared with free DOX. Wang *et al.* [22] similarly designed a CDs-DOX delivery system, which prolonged the circulation time of DOX in the blood and exhibited an excellent *in vivo* antitumor effect in mice with HepG2 subcutaneous transplanted tumors. The present CDs can improve drug-targeted ability to tumor tissues through EPR effect, but just at the tissue and cellular level. Therefore, the concentration of drugs that enter the nuclei is limited, resulting in the inability to improve tumor efficacy fundamentally.

It is an effective way for precise and efficient nucleus-targeting drug delivery to improve the efficacy of DOX. Researchers usually use electrostatic self-assembly and targeting molecular modification to endow CDs with nucleus-targeting ability [23,24]. Nuclear localization sequence (NLS) is one of classical nuclear localization molecules, and often used to mediate the nucleus-targeting chemotherapy in tumors. After modification of NLS on CDs, they can successively bind to nuclear import proteins α/β in the cytoplasm and eventually form dimers, and then direct to the nucleus through the nuclear pore complex [25]. In recent years, the anti-tumor research of NLS as a nucleus-targeting molecule has achieved desirable effect. Yang *et al.* [26] prepared nucleus-targeting CDs using NLS as a targeting molecule, and constructed a targeted drug delivery anti-tumor system by coupling DOX, which achieved better anti-tumor efficacy than the control group both *in vitro* A549 cells and *in vivo* tumor-bearing mice. Chen *et al.* [27] prepared the liposomal nanoparticles encapsulating CD-DOX in this way, avoiding their clearance by the immune system *in vivo*, and indicated that the precise nucleus targeting enabled CD-DOX to exhibit ideal *in vivo* antitumor effects.

It is clear that a variety of nanoparticles modified with NLS have achieved fruitful results. However, with precise guidance of NLS, the current nucleus targeted CDs loaded with chemotherapeutic drugs for antitumor therapy are mostly concentrated in the short wavelength (blue and green) emission region, which cannot avoid biological autofluorescence interference and may cause damage to tissues and cells. The long wavelength emissive CDs for targeting nuclei can improve the depth of tissue penetration, which is important for the fluorescence tracing of drugs, the feedback of treatment effect, and the integration of diagnosis and treatment. However, the studies on long-wavelength emissive CDs for targeting the nuclei in antitumor are rarely reported, which greatly limits the effectiveness of nucleus-targeting CDs in cell imaging and drug delivery.

To this end, in order to improve the precise chemotherapy effect for liver cancer, this paper designs and constructs a nucleus-targeting nano-drug delivery complex using long-wavelength emissive CDs as carrier to deliver antitumor drug DOX under the help of NLS (Scheme 1). Currently, the main strategies for preparing long-wavelength emissive CDs include doping heteroatoms, increasing conjugation length, and surface functionalization or

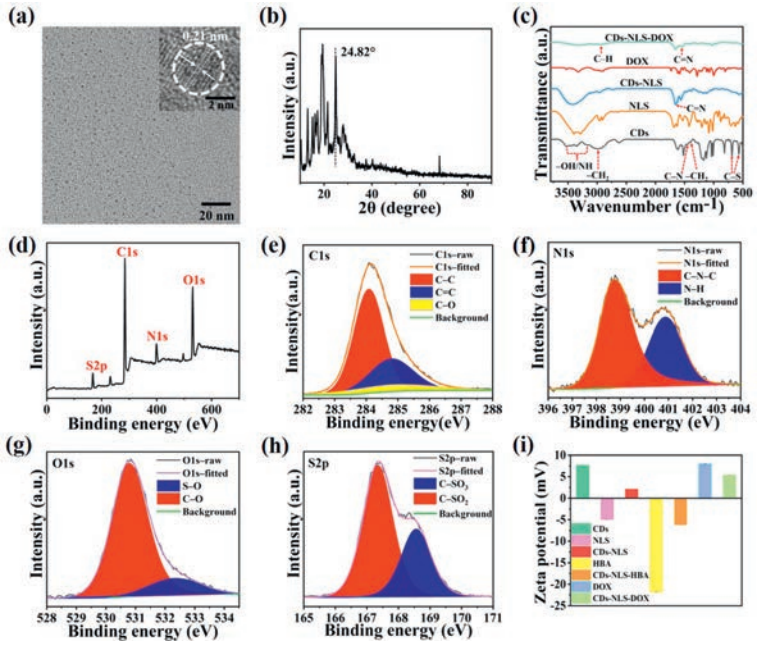

Fig. 1. Structural and compositional characterization. (a) TEM image of CDs, HRTEM image in the upper right corner. (b) XRD patterns of CDs. (c) FT-IR spectra of CDs, NLS, CDs-NLS, DOX, and CDs-NLS-DOX. (d) Full XPS spectrum of CDs. High-resolution XPS peaks of (e) C 1s, (f) N 1s, (g) O 1s, (h) S 2p. (i) Zeta potential.

passivation [28,29]. Inspired by the above preparation strategies, one of main feature of this paper is to use a simple one-step solvothermal method to realize long wavelength orange emissive CDs with the aid of doping nitrogen/sulfur heteroatoms and increasing conjugation structure, in which *p*-phenylenediamine (PD) and *p*-toluenesulfonic acid (TSA) were used as raw materials. Another feature lies in coupling NLS on the surface of the CDs to obtain nucleus-targeting CDs (CDs-NLS). In order to load DOX onto CDs-NLS through pH-sensitive acylhydrazone bonds, the hydrazine group was first introduced with *p*-carboxyphenylhydrazine (HBA) as an intermediate, followed by loading DOX on CDs, to achieve the nucleus-targeting long-wavelength emissive CDs delivery system (CDs-NLS-DOX). Nucleus-targeting imaging was used for detecting the development of live cancer *in vitro*. CDs-NLS-DOX selectively accumulate at the tumor site through EPR effect, and subsequently targeted deliver DOX to the nucleus. DOX can be released under the tumor acidic microenvironment owing to the pH-responsive acylhydrazone bonds to inhibit the proliferation of cancer cell. By exploring the morphological structure and optical properties of CDs, evaluating the cellular uptake and nuclear targeting ability of CDs-NLS, examining its DOX loading efficiency and release characteristics, and performing *in vitro* and *in vivo* proliferation inhibition investigation and histological analysis on liver cancer cells and HepG2-bearing mice, the efficient anti-tumor effect of CDs-NLS-DOX drug delivery complex were validated. This work provides a new strategy for targeted chemotherapy of cancer.

First, the morphology and particle size of the CDs were observed and analyzed. Transmission electron microscopy (TEM) image and the particle size distribution map (Fig. 1a and Fig. S1 in Supporting information) show that the CDs are torispherical with an average diameter of about 2.36 ± 0.49 nm, which is normally distributed and uniformly dispersed. The high-resolution TEM (HRTEM) image in the upper right corner of Fig. 1a shows that the CDs have distinct lattice stripes with an average lattice spacing of about 0.21 nm, corresponding to the crystalline plane of graphite (100) [30]. As shown in Fig. 1b, a narrow diffraction peak at 24.82° is attributed to the (002) crystalline plane of graphitic carbon. Moreover, some sharp narrow peaks are originated from the ordered polymeric cross-linked structure of the CDs. It demonstrates that CDs have ordered carbonized polymer around with their graphitic carbon cores [31].

To determine the structures of the products at each stage, the surface states of CDs, CDs-NLS and CDs-NLS-DOX were investigated by using Fourier transform infrared spectroscopy (FT-IR). As shown in Fig. 1c, the broad vibrational bands in the range of 3196–3527 cm^{-1} in CDs are attributed to the –OH/NH vibrations, and the bands at 2991 and 1394 cm^{-1} are attributed to the vibrations of $-CH_2$. These functional groups demonstrate that CDs have good water solubility, which is favorable for subsequent DOX loading [32]. In addition, the appearance of 1460 cm^{-1} absorption peaks in CDs and CDs-NLS is attributed to the C–N vibrations, and the absorption peaks at 567 and 680 cm^{-1} are due to C–S vibrations. Moreover, a new absorption peak at 1649 cm^{-1} appears in CDs-NLS, which represents the characteristic absorption band of C = N bond in NLS, suggesting that the surface of CDs is modified by NLS [24,27]. Furthermore, the FT-IR spectrum of CDs-NLS-DOX is also presented in Fig. 1c. The absorption peak at 3294 cm^{-1} is due to the tensioning vibration of –OH/NH, and the new bands at 2935 and 1546 cm^{-1} correspond to the tensioning vibration of the C–H group in the pyran ring and the stretching vibration of C=N in the hydrazone bond in DOX, respectively. It demonstrates the acid-sensitive acylhydrazone bond is generated on CDs, and drug delivery system CDs-NLS-DOX are well synthesized [26].

In addition, the internal elemental composition and surface states of CDs were characterized by X-ray photoelectron spectroscopy (XPS), which further verifies FT-IR characterization results. As shown in Fig. 1d, the XPS results indicate that the CDs contain four elements: carbon, nitrogen, oxygen, and sulfur. The high-resolution spectra of each element were tested separately (Figs. 1e–h). The high-resolution spectrum of C 1s (Fig. 1e) can be fitted to three peaks, and they are C–C (284.08 eV), C=C (284.80 eV) and C–O (285.01 eV) groups, respectively [33]. The N atoms (Fig. 1f) exist in the form of C–N–C (398.71 eV) and N–H bonds (400.86 eV) [34]. The two peaks of O 1s spectrum (Fig. 1g) are attributed to C–O (530.77 eV) and S–O (532.34 eV) [34,35]. The S 2p spectrum (Fig. 1h) shows two peaks at 167.35 and 168.56 eV, which correspond to $C–SO_2$ and $C–SO_3$ bonds, respectively [36,37].

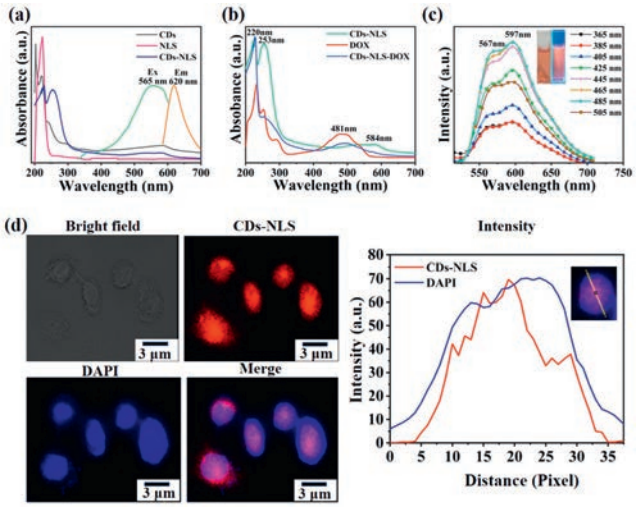

Fig. 2. (a) UV–vis absorption spectra of CDs, NLS, CDs-NLS and excitation and emission spectra of CDs. (b) UV–vis absorption spectra of CDs-NLS, DOX, CDs-NLS-DOX. (c) Emission spectra of CDs-NLS-DOX at different excitation wavelengths. (d) Fluorescence micrographs of CDs-NLS after co-culture with HL-7702 cells for 6 h: bright field, fluorescence, 4,6-diamino-2-phenyl indole (DAPI), overlap images and fluorescence intensity profiles.

The XPS results confirmed the presence of surface amino groups on CDs. Zeta potential results demonstrates CDs-NLS-DOX with positive charge was obtained (Fig. 1i), which is more likely to bind into the intracellular area to exert anti-tumor effects (as illustrated in Supporting information 2.1) [38].

The optical properties of materials are crucial for their applications in bioimaging and drug delivery. Therefore, to understand the optical properties of as-prepared CDs, CDs-NLS and CDs-NLS-DOX, the ultraviolet–visible (UV–vis) and photoluminescence (PL) spectra of all three products were tested. As shown in Fig. 2a, the CDs in aqueous solution have distinct absorption peaks at 203, 220 and 584 nm. Among them, the absorption bands at 203 and 220 nm in the UV region are attributed to the π-π^* leap of aromatic C=C, and the absorption peak near 584 nm in the visible light region is the typical absorption band of aromatic structures, indicating a large conjugate structure in CDs [39–41].

In addition, CDs-NLS inherits the original absorption peak of CDs at 584 nm, and the appearance of the NLS absorption peak at 223 nm also indicates the conjugation of CDs with NLS. Moreover, as shown in Fig. 2b, the appearance of the characteristic absorption peak of DOX at 481 nm in CDs-NLS-DOX and the retention of the absorption peaks of CDs-NLS at 220, 253 and 584 nm, indicating the successful loading of DOX on CDs-NLS. Fig. 2c shows the PL spectra of the CDs-NLS-DOX. Two excitation-independent emission peaks are visible and located at 567 and 597 nm, respectively. Since the emission peak of DOX at the optimal excitation wavelength is located at 575–585 nm, while the emission peak of CDs-NLS is located at 615 nm (Fig. S2b in Supporting information), it can be seen that the emission peaks of both DOX and CDs-NLS in the drug-loading complex are blue-shifted. This phenomenon of blue-shifted emission wavelengths in the complex has been reported in the literature, which can be attributed to the combination of two substances [29]. Moreover, CDs also have good stability in different pH environments (Fig. S2c in Supporting information), and can be used for biolabeling and imaging.

To assess the ability of CDs-NLS targeting to the nucleus as a drug carrier, their fluorescence imaging was performed on HL-7702 and VX2 cells using CDs as a control (Fig. 2d, Figs. S3 and S4 in Supporting information). As shown in Fig. 2d, the orange-red fluorescence of HL-7702 cells cultured with CDs-NLS is mainly localized to the nucleus and become pink by fusing with the blue fluorescence of the nuclear dye DAPI. It is also clearly observed in the pixel intensity distribution map that the signal of CDs-NLS show significant overlap with DAPI. In contrast, the orange-red fluorescence of CDs is mainly localized in the cytoplasm with no obvious co-localization with the nucleus (Fig. S3), as reflected in the pixel intensity distribution map. The results in VX2 cells are the same (Figs. S3 and S4). Therefore, CDs can be effectively transferred from the cytoplasm to the nucleus for fluorescence imaging by NLS-mediated active transport, and the drugs they carry can be precisely targeted to the nucleus, promising the integration of diagnosis and treatment.

The toxicity of CDs, as the potential drug carrier materials for biomedical applications, has been of great concern. Figs. S5a and b (Supporting information) show the *in vitro* cytotoxicity of CDs and CDs-NLS after 24 h incubation with HL-7702, VX2 and HepG2 cells, respectively. All three solutions show good cell activity at a concentration of 200 μg/mL, which is greater than 80%. The survival rates of all three cells are higher than 75% even when incubated at a much higher working concentration of 400 μg/mL. These results indicate that CDs and CDs-NLS have low cytotoxicity to cells after incubating up to 24 h at a wide range of concentrations. Significantly, at lower concentrations, the viability of some cells exceeds 100%, which is obviously higher than that of the control group, suggesting that low concentrations of CDs and CDs-NLS may actually promote cell proliferation, which may be due to the nanocarriers stimulating cell growth and promoting proliferation or differentiation by constructing scaffolds [42]. In addition, the toxicity of CDs and CDs-NLS as drug carriers was also fully investigated by *in vivo* 7 and 21 days studies. The results indicate that the prepared drug carriers have less systemic toxicity and can be used for *in vivo* (Figs. S6 and S7 in Supporting information).

The CDs-NLS-DOX complexes, which were obtained by CDs-NLS bonding with DOX through acid-sensitive acylhydrazone bonds, can avoid the early release of DOX during the blood delivery, achieving the controlled release of DOX. The DOX loading capacity of CDs-NLS-DOX complexes were in valuated and optimized. A drug loading efficiency (DLE) of 59.4% was obtained when the mass ratio of CDs-NLS-HBA and DOX was 4:1, and the complex has higher release of DOX under weakly acidic conditions (Fig. S8 in Supporting information), which can be explained by the breakage of hydrazone bonds in the molecule, suggesting that the complex can selectively release the drug under acidic environments, which is beneficial for the effective treatment of cancer.

The proliferation inhibition of HepG2 cells incubated with free DOX, CDs-DOX and CDs-NLS-DOX for 24 h was investigated to assess the *in vitro* antitumor activity. As can be clearly observed in Fig. 3a, the toxicity of all three groups against HepG2 cells gradually increases with increasing DOX drug concentration, showing a dose-dependent death. The overall inhibition shows CD-NLS-DOX > CDs-DOX > free DOX. At DOX doses of 0.3125, 2.5, 10 and 20 μg/mL, compared with free DOX, CDs-NLS-DOX group shows relatively higher cytotoxicity with significant differences, which have statistically significant ($P < 0.05$). Especially, when the concentration of DOX is increased to 20 μg/mL, the cell survival rate of CDs-NLS-DOX-treated cells is only 18.0%, while the survival rate of free DOX group is 42.5% at this time, demonstrating a stronger tumor-killing effect. Further, it is observed that the inhibition of the CDs-DOX group for HepG2 proliferation is higher than that of the free DOX group at all concentrations, but it is significantly lower than that of the CDs-NLS-DOX group at equivalent DOX concentrations. These results suggest that CDs-DOX group can induce much DOX entry into the cell to some extent compared with the free DOX group. Without NLS-mediated nucleus-targeting drug delivery, DOX is mostly localized in the cytoplasm, which fails to adequately increase its contact with DNA in the nucleus. Therefore, CDs-NLS-

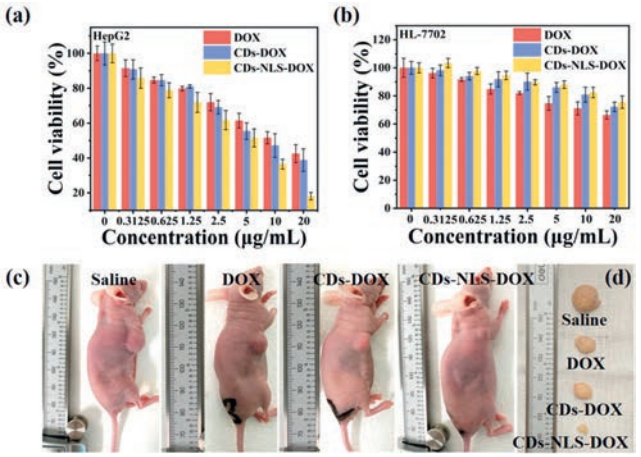

Fig. 3. Antitumor activity of DOX, CDs-DOX and CDs-NLS-DOX *in vitro* on (a) HepG2 and (b) HL-7702, values are expressed as mean ± standard deviation ($n = 3$). (c) Representative photographs of mice at 15 days after treatment. (d) Images of resected tumors.

DOX exerts an enhanced tumor-killing effect compared with the other two groups.

However, the cytotoxicity results in normal hepatocytes (HL-7702) treated with free DOX, CDs-DOX and CDs-NLS-DOX are in marked contrast to HepG2 cells. As shown in Fig. 3b, the cytotoxicity of CDs-NLS-DOX group is significantly smaller than that of both free DOX and CDs-DOX groups at the same concentration, with almost no cytotoxicity, reflecting the protection of normal cells. The survival rate of HL-7702 cells is close to 80% even at a DOX drug concentration as high as 20 μg/mL, while the survival rates of free DOX and CDs-DOX groups show cell survival rates of 72% and 68%, respectively. Moreover, only a DOX concentration of 2.5 μg/mL free DOX can kill 20% of HL-7702 cells, suggesting that the damage of free DOX to HL-7702 cells is greater. The above *in vitro* toxicity results show that CDs-NLS-DOX group has a stronger killing effect on hepatocellular carcinoma cells compared with the free DOX and CDs-DOX groups. To some extent, it can protect normal cells from the side damage caused by the indiscriminate distribution of chemotherapeutic drugs.

Based on the good apoptosis-inducing ability of CDs-NLS-DOX *in vitro*, a tumor-bearing mouse model was established by subcutaneous inoculation of HepG2 cells to evaluate *in vivo* targeted anti-tumor activity. All the animal experiments were approved by the Experimental Animal Ethics Committee of Shanxi Medical University. Figs. 3c and d are the representative photos of nude mice and resected tumors after 15 days treatment. It can be found that compared with the saline group, CDs-NLS-DOX group has the same inhibitory effect on tumor growth as the CDs-DOX and free DOX groups, but the CDs-NLS-DOX group has the best inhibitory effect on tumor, which is verified that the tumor is significantly reduced or even completely disappeared.

The analysis of tumor growth curve and weight (Figs. S9a and b in Supporting information) also demonstrated that CDs-NLS-DOX has a stronger tumor suppression effect than other groups. On the one hand, the enhanced antitumor effect may be due to the EPR effect of solid tumors which allows more drug accumulation at the tumor site. On the other hand, owing to the nucleus-targeting guidance of NLS, the therapeutic effect can be efficiently achieved by targeted drug delivery and acid environment responsive drug release. Moreover, to investigate the efficacy and systemic toxicity of DOX on tumors in nude mice at the end of treatment, the histological changes in the CDs-NLS-DOX group were observed after treatment. Tumors and major organs such as heart, liver, spleen, lung and kidney were collected from the CDs-NLS-DOX group for hematoxylin-eosin (HE) staining analysis (Fig. S9c in Supporting information), it proves the high efficiency and low toxicity of CDs-NLS-DOX in killing tumors, reflecting the potential application prospects of CDs-NLS-DOX nucleus-targeting drug delivery system.

In summary, in order to improve the existing shortcomings such as the non-differential distribution of drugs and the occurrence of multidrug resistance during clinical liver cancer chemotherapy, the orange-emissive CDs with an emission wavelength of 620 nm and a fluorescence quantum yield of 17.3% were firstly prepared by solvothermal method using *p*-phenylenediamine and *p*-toluenesulfonic acid as raw materials. Obtained CDs have an average particle size of 2.36 ± 0.49 nm, uniform distribution, abundant amino and hydroxyl functional groups on the surface, and good water solubility. Subsequently, a novel nucleus-targeting drug delivery system CDs-NLS-DOX was obtained based on the covalent coupling of NLS and DOX with CDs as the drug carrier. The appearance of overlapping fluorescence in the nucleus indicated that CDs-NLS was accurately localized in the nucleus after entering the cells, realizing the precise nucleus-targeting imaging. In the acidic environment, the CDs-NLS-DOX drug delivery system exhibited environmentally responsive DOX release, which was 57.98% more than that in the neutral environment. In an *in vitro* HepG2 cell inhibition assay, free DOX, CDs-DOX and CDs-NLS-DOX showed a dose-dependent killing effect, with the cell survival ability at only 18.0% of CDs-NLS-DOX group, 42.5% of DOX group, and 38.3% of CDs-DOX at a concentration of 20 μg/mL, respectively. The higher survival rate for CDs-NLS-DOX confirms that it has a more pronounced tumor suppressive effect than free DOX and CDs-DOX. The difference in HL-7702 cell activity also indicates that CDs-NLS-DOX can protect normal cells from side effects caused by the indiscriminate distribution of chemotherapeutic drugs to some extent. Notably, *in vivo* treatment effect also confirms the enhanced tumor growth inhibitory ability of CDS-NLS-DOX complexes. In conclusion, the CDs-NLS-DOX obtained in this study is expected to be a candidate for tumor nucleus-targeting drug delivery and has great potential for cancer chemotherapeutic applications.

Declaration of competing interest

The authors declare that they have no known competing financial interests or personal relationships that could have appeared to influence the work reported in this paper.

Acknowledgments

This work was supported by the National Natural Science Foundation of China (Nos. 82172048 and U21A20378), Scientific Research Project of Shanxi Provincial Health Commission (No. 2023120), Shanxi-Zheda Institute of Advanced Materials and Chemical Engineering (No. 2021SX-FR010), Shanxi Center of Technology Innovation for Controlled and Sustained Release of Nanodrugs (No. 202104010911026), Foundational Research Project of Shanxi Province (No. 202203021211159), Four "Batches" Innovation Project of Invigorating Medical through Science and Technology of Shanxi Province (No. 2023XM012), and Shanxi Scholarship Council of China (No. 2022–039).

Supplementary materials

Supplementary material associated with this article can be found, in the online version, at doi:10.1016/j.cclet.2023.108947.

References

[1] M. Feng, Y. Pan, R. Kong, S. Shu, Innovation 1 (2020) 100032.
[2] Z. Liu, Y. Jiang, H. Yuan, et al., J. Hepatol. 70 (2019) 674–683.

[3] J. Tang, R. Zhang, M. Guo, et al., J. Control. Release 320 (2020) 293–303.
[4] X. Yang, X. Yang, P. Luo, et al., Mater. Today Bio 20 (2023) 100688.
[5] C. Qiu, Y. Wu, Q. Guo, et al., Mater. Today Bio 17 (2022) 100501.
[6] L. Wang, X. Niu, Q. Song, et al., J. Control. Release 318 (2020) 197–209.
[7] X. Hua, Y. Bao, F. Wu, ACS. Appl. Mater. Interfaces 10 (2018) 10664–10677.
[8] J. Xin, S. Wang, J. Wang, et al., J. Biomed. Nanotechnol. 18 (2022) 837–848.
[9] W. Pang, P. Jiang, S. Ding, et al., Adv. Healthc. Mater. 9 (2020) e2000607.
[10] A. Yaghoubi, A. Ramazani, J. Control. Release 327 (2020) 198–224.
[11] P. Laskar, S. Somani, S.J. Campbell, et al., Nanoscale 11 (2019) 20058–20071.
[12] M. Bar-Zeev, Y.D. Livney, Y.G. Assaraf, Drug Resist. Updat. 31 (2017) 15–30.
[13] C. Duan, S. Li, X. Wang, T. Lu, J. Int. Pharm. Res. 5 (2018) 899–904.
[14] L. Wang, B. Wang, E. Liu, et al., Chin. Chem. Lett. 33 (2022) 4111–4115.
[15] X. Yang, X. Li, B. Wang, et al., Chin. Chem. Lett. 33 (2022) 613–625.
[16] A. Lv, Q. Chen, C. Zhao, et al., Chin. Chem. Lett. 32 (2021) 3653–3664.
[17] C. Carvalho, R.X. Santos, S. Cardoso, et al., Curr. Med. Chem. 16 (2009) 3267–3285.
[18] C.F. Thorn, C. Oshiro, S. Marsh, et al., Pharmacogenet. Genom. 21 (7) (2011) 440–446.
[19] W. Zhou, Z. Hu, J. Wei, et al., Chin. Chem. Lett. 33 (2022) 1245–1253.
[20] M. Sharifi, W.C. Cho, A. Ansariesfahani, et al., Cancers 14 (2022) 2868.
[21] T. Kong, L. Hao, Y. Wei, X. Cai, B. Zhu, Cell Prolif. 51 (2018) e12488.
[22] S. Wang, L. Chen, J. Wang, et al., Mater. Sci. Eng. C Mater. Biol. Appl. 116 (2020) 111233.
[23] S. Chen, X. Zhang, Y. Yu, J. Wang, Chin. Chem. Lett. 32 (2021) 3043–3047.
[24] G. Zou, S. Chen, N. Liu, Y. Yu, Chin. Chem. Lett. 33 (2022) 778–782.
[25] S. Kosugi, M. Hasebe, N. Matsumura, et al., J. Biol. Chem. 284 (2009) 478–485.
[26] L. Yang, Z. Wang, J. Wang, et al., Nanoscale 8 (2016) 6801–6809.
[27] W. Chen, J. Li, Y. Xing, et al., Pharm. Res. 37 (2020) 134.
[28] C.L. Shen, H.R. Liu, Q. Lou, et al., Theranostics 12 (2022) 2860–2893.
[29] Y. Yuan, B. Guo, L. Hao, et al., Colloids Surf. B: Biointerfaces 159 (2017) 349–359.
[30] Y. Ding, J. Zheng, J. Wang, Y. Yang, X. Liu, J. Mater. Chem. C (2019) 1502–1509.
[31] C. Ji, Q. Han, Y. Zhou, et al., Carbon 192 (2022) 198–208.
[32] S. Lei, N. Chang, J. Zhang, H. Wang, Anal. Sci. 37 (2021) 851–857.
[33] Z. Mua, J. Hua, Y. Yang, Spectrochim. Acta A Mol. Biomol. Spectrosc. 224 (2020) 117444.
[34] C. Shi, H. Qi, R. Ma, et al., Mater. Sci. Eng. C Mater. Biol. Appl. 105 (2019) 110132.
[35] K.M. Tripathi, H.T. Ahn, M. Chung, et al., ACS Biomater. Sci. Eng. 6 (2020) 5527–5537.
[36] Y. Wang, L. Yan, G. Ji, et al., ACS Appl. Mater. Interfaces 11 (2019) 2243–2253.
[37] B. Wang, Z. Wei, L. Sui, et al., Light Sci. Appl. 11 (2022) 172.
[38] V.K. Bajpai, I. Khan, S. Shukla, et al., Theranostics 10 (2020) 7841–7856.
[39] Y. Jiao, Y. Liu, Y. Meng, et al., ACS Sustain. Chem. Eng. 8 (2020) 8585–8592.
[40] R. Fu, H. Song, X. Liu, et al., Chin. J. Chem. 41 (2023) 1007–1014.
[41] Y. Jiao, Y. Meng, W. Lu, C. Dong, et al., Talanta 219 (2020) 121170.
[42] T. Gong, J. Xie, J. Liao, et al., Bone Res. 3 (2015) 15029.